ISSN (Online) 2456-1290

International Journal of Engineering Research in Mechanical and Civil Engineering (IJERMCE)

Volume 13, Issue 03, March 2026

Design and Structural Analysis of an Aerial Cable Transport Cabin

[1] Kanishk Tiwari, [2] Rajeev Kumar, [3] M. Talha

[1] [2] [3] School of Mechanical and Materials Engineering, Indian Institute of Technology Mandi, Himachal Pradesh, India
Corresponding Author Email: [1] pts2403@students.iitmandi.ac.in

Abstract*— Urban ropeway transport systems require passenger cabins that are both lightweight and structurally dependable to ensure safe operation under various service conditions. Designing such cabins is challenging because they must withstand the combined effects of passenger loads, strong winds, hail impact and dynamic forces during station entry, while still maintaining sufficient strength, stiffness and overall safety within a compact structural layout. This paper presents a detailed structural design and assessment of the critical load-bearing components of a newly developed ten-passenger aerial ropeway cabin, carried out in line with international safety standards. All essential operational and environmental loads including the self-weight of the structure, non-structural components, passenger loading, wind action, hail impact and dynamic forces during station entry have been carefully evaluated and applied to the structural model. The cabin frame and the coupling element support are designed using Aluminum 6061-T6, while the H-bracket is fabricated from ASTM A572 Grade 50 steel. Finite element analysis is carried out to evaluate deformation, von Mises stress response and factors of safety of the critical structural components under the governing load combinations. The H-bracket is found to experience a maximum stress of 66.20 MPa with a safety factor of 5.21. All result values remain well within elastic limits, confirming compliance with international design standards and validating that the proposed critical component configuration is lightweight, structurally safe, and suitable for manufacturability, prototype development and integration into urban ropeway systems.

Index Terms*— Aerial cable transport, finite element analysis, H-bracket, ropeway cabin, structural design, Dynamic Load Evaluation, Urban Ropeway Systems.

I. INTRODUCTION

Urban centers have faced increasing challenges related to congestion, limited infrastructure and rising environmental concerns which have led cities to explore alternative and sustainable transportation solutions. Aerial cable transport systems have gained significant attention as they provide efficient mobility with minimal land use, low energy consumption and reduced emissions. Initially used for mountainous regions, these systems have been adopted in urban environments as reliable and practical modes of passenger transport. Fundamental principles of ropeway cabin design, including aerodynamic stability and structural performance, follow the guidelines discussed in [10]. An aerial ropeway typically consists of three main subsystems: the traction system, which drives the cable, the support system, comprising towers and foundations and the loading system, which includes the passenger cabin and its structural connections. Among these, the cabin assembly has represented a critical element because it directly affects passenger comfort, operational safety, and overall system reliability, as noted in earlier studies [4] and in safety guidelines such as UNE-EN 12929-1 [5]. Wind-induced oscillations and cross-wind effects have been shown to cause significant lateral sway and vibration in ropeway cabins, directly influencing passenger comfort and structural safety [11]. The dynamic behavior of aerial cableway systems under moving loads, including acceleration and braking, has also been investigated, demonstrating that these effects generate substantial additional forces in cabin suspension and hanger components [12]. Further studies on detachable ropeway systems exposed to wind loads have reported that the combined action of aerodynamic and inertial forces governs the stress state of cabin–hanger assemblies during operation [13]. More recent research has confirmed that finite element analysis is an effective and reliable tool for evaluating deformation, stress distribution, and safety factors of critical mechanical components in cable-car and ropeway systems prior to manufacturing [14].

The present study has focused on designing and assessing a ten-person aerial transport cabin using finite element analysis (FEA). The structural verification has been carried out in accordance with the requirements of UNE-EN 13796-1 [1]. The work has examined three major structural components the cabin frame, the H-bracket and the coupling element support “H” to ensure effective load transfer, sufficient stiffness and high safety margins under operational and environmental loading conditions. The outcomes of this study have contributed to the development of lightweight and structurally reliable cabin configurations suitable for urban ropeway applications, supporting the advancement of sustainable aerial mobility systems.

In this article, Section II describes the design methodology, load evaluation, material selection, and finite element modeling of the critical structural components of the ropeway cabin. Section III presents the numerical results, including deformation, stress distribution, and factor of safety for the cabin frame, H-bracket, and coupling element support. Section IV discusses the key findings and their

ISSN (Online) 2456-1290

International Journal of Engineering Research in Mechanical and Civil Engineering (IJERMCE)

Volume 13, Issue 03, March 2026

structural implications. Finally, Section V summarizes the main conclusions of the study.

II. AERIAL TRANSPORT CABLE CABIN

The aerial transport cable cabin is the primary passenger-carrying unit of the ropeway system and is designed to ensure passenger safety, comfort, structural reliability, and compliance with UNE-EN 13796-1 [1]. The proposed cabin is intended to accommodate ten passengers and is developed with a lightweight yet sufficiently stiff structural configuration to withstand operational and environmental loads.

The cabin structure is designed to provide adequate floor area for passenger comfort while maintaining compact geometry suitable for aerial transport applications. Key characteristics of the proposed cabin include a lightweight aluminum frame, efficient load transfer through the coupling, H-bracket assembly and the provision of damping elements to reduce vibration during operation. The proposed aerial transport cable cabin configuration is shown in Fig. 1. The present design has accommodated ten passengers, maintaining lightweight structure and adequate rigidity.

The overall arrangement has been developed following the methodology described by Villarreal et al. [4], in which the effective cabin floor area (superficies) is expressed in eq. 1 as a function of the number of passengers (n):

$$A\ (Superficies) = 0.5 + a \times n \qquad (1)$$

Where:

A (superficies) = effective cabin floor area (m²),

a = empirical area coefficient (0.15 to 0.25) m²

n = number of passengers

Using the empirical area coefficient, $a = 0.20 m^2/person$ and $n = 10$ passengers, the resulting effective area is:

$$A(Superficies) = 0.5 + (0.20 \times 10) = 2.5 m^2.$$

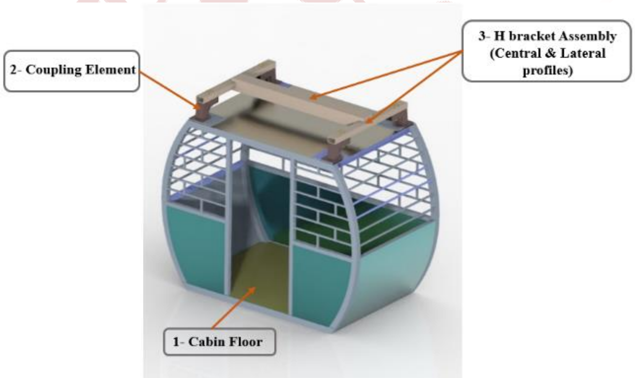

Figure 1. Aerial transport cable cabin

This surface dimension aligns with the configuration proposed in [4], ensuring sufficient space for passenger comfort while maintaining compact geometry suitable for ropeway operation. The main cabin frame has been constructed from $Aluminum\ Alloy\ 6061 - T6$, while the H-bracket connecting the cabin to the suspension system has been fabricated using ASTM A572 Grade 50 steel [3]. The coupling element (support H) manufactured from $Aluminum\ 6061 - T6$, has served as the interface with the damping system and has transmitted the dynamic reaction forces that occur during station entry and exit. This component has represented one of the most critical regions due to its susceptibility to stress concentration. A four-spring damping system has been incorporated to reduce vibration and lateral oscillations during operation. The resulting cabin configuration has formed the structural basis for the finite element analysis conducted in ANSYS R1 2024 to verify deformation, stress levels, and safety margins under all governing load cases.

III. METHODOLOGY

The engineering design and validation of the ten-person aerial cabin has been carried out using a structured procedure consistent with the method proposed by Villarreal et al. (2021) and in accordance with the requirements of UNE-EN 13796-1 [1] for passenger cableway systems. The methodology has involved defining the governing design parameters, establishing all operational and environmental load conditions, examining the behavior of the damping and connection systems and performing structural verification through finite-element analysis (FEA) in ANSYS R1 2024.

This integrated approach has ensured that each component of the cabin assembly has been evaluated under realistic service conditions, allowing the design to be assessed for stiffness, strength, and safety in compliance with international standards. Similar finite-element modelling approaches for ropeway cabin structures have been demonstrated in [8], which further supports the methodology followed in the present work.

3.1.1. Design Parameters

The principal design parameters have been established based on environmental and operational conditions that influence the cabin's structural behavior. The selected loading conditions have followed those adopted by Villarreal et al. [6] and comply with the safety provisions of UNE-EN 13796-1 [1].

3.1.2 Design Loads

- Dead load (G): Self-weight of the cabin's structural members
- Non-structural load (G_1): Weight of all non-structural components, including interior panels, handrails, fittings, glazing and miscellaneous accessories that contribute additional static mass to the cabin assembly.
- Passenger load (Q): Ten passengers, each with an average design mass of 80 kg as stipulated in UNE-EN 13796-1 [1], which includes allowance for clothing and personal belongings. The total passenger mass of 800 kg is applied as a uniformly distributed load over the cabin floor.

ISSN (Online) 2456-1290
International Journal of Engineering Research in Mechanical and Civil Engineering (IJERMCE)
Volume 13, Issue 03, March 2026

- Wind load (F_w): derived from the regional maximum velocity of 70.4 km/h (19.6 m/s) as reported in the hydrometeorological study by EMMOP [7].
- Hail load (S): Defined as 1.0 kN/m², representing a heavy hail condition in accordance with the Ecuadorian Construction Standard NEC-SE-CG [2].
- Dynamic reaction (R): determined according to UNE-EN 13796-1 [1], representing the deceleration forces acting on the coupling interface during cabin entry and exit from the station.

3.1.3 Evaluation of Design Loads

The evaluation of design loads has been carried out following the analytical relations established in UNE-EN 13796-1 [1] and the procedure described by Villarreal et al. [6]. The same methodological framework has been applied to the present cabin design, with all calculations performed using the specific geometric and loading parameters of the newly developed ten-passenger cabin.

Wind Load

The wind pressure acting on the exposed surfaces of the cabin has been evaluated using the standard aerodynamic wind-pressure relation adopted by Villarreal et al. [6] in accordance with the operational requirements of UNE-EN 13796-1 [1].

$$q = 0.613\, V^2 \text{ [16]} \tag{2}$$

where
q = wind pressure (N/m²),
q_{red} = reduced wind pressure (N/m²),
V = Wind Velocity(m/s).

For the present study, the regional design velocity was taken as $V = 19.56 m/s$ (equivalent $70.4\ km/h$) has been adopted based on the hydrometeorological data provided by EMMOP [7]. Substituting this velocity into the equation gives:

$$q = 0.613\, x\, (19.56)^{2} = 234.5 N/m^2$$

The basic pressure q is multiplied by the coefficient $\beta = 1.0$ as specified in UNE-EN 13796-1 [1] defined in eq. 3, yielding the reduced design wind pressure:

$$q_{red} = \beta\, q = 234.5 \text{ N/m}^2 \tag{3}$$

This pressure value is used in the finite-element model of the current cabin to represent wind loading conditions.

Hail Load

The hail load acting on the cabin roof and upper panels are determined using the procedure outlined in the Ecuadorian Construction Standard NEC-SE-CG [2] and following the methodology adopted by Villarreal et al. [6]. The load is defined in eq. 4:

$$S = q_s \times H_s \tag{4}$$

where
S = hail load (kN/m²)
q_s= hail density (kg/m³),
H_s= accumulation height (m).

For conservative design under heavy hail conditions, the accumulation height has been taken as $q_s = 1000\ kg/m^3$ and H_s = 0.001m, the resulting hail load as data provided by EMMOP [7]:

$$S = 1000 \times 0.001 = 1.0 kN/m^2$$

This uniform surface pressure is applied to the roof and upper panels of the cabin model. The same design approach has been used by Villarreal et al. [6] in validating aerial cable transport cabin structures.

Considering the exposed roof area of the cabin, = 2.632 m^2(present cabin Roof area), the total hail load applied in the finite element model is:

$$F = S \times A = 1.0 \times 2.632 = 2.632 kN$$

This load intensity and its uniform distribution are consistent with the methodology reported in [6] and have been applied across all horizontal and moderately inclined upper surfaces of the cabin.

Dynamic Reaction Force

In addition to the static and environmental loads, the cabin has been subjected to a dynamic reaction force at the coupling interface during station entry and exit. This force represents the deceleration effect as the cabin transitions from motion to rest, has been evaluated according to the formulation specified in UNE-EN 13796-1 [1], following the same principle applied by Villarreal et al. [6] as defined in eq. 5:

$$F = \frac{mV}{t} \tag{5}$$

Where
$F = reaction\ force\ (N)$,
$m = total\ loaded\ mass\ (kg)$,
$V = entry\ velocity\ \left(\frac{m}{s}\right)$,
$t = deceleration\ time\ (s)$.

For the present designed ten-passenger cabin, the total loaded mass has been as $m = 1300\ kg$, the entry velocity $V = 2m/s$, and the deceleration time $t = 0.8s$. Substituting these values gives:

$$F = 1300 \times 2/0.8 = 3250\ N$$

This calculated dynamic reaction force of 3250 N is applied at the coupling interface in the structural analysis. The higher total load of 18306.4 N used in the critical load combination (Villarreal et al. [6]) reflects additional safety margins and conservative assumptions for simultaneous loading conditions, maintaining consistency with the

ISSN (Online) 2456-1290

International Journal of Engineering Research in Mechanical and Civil Engineering (IJERMCE)

Volume 13, Issue 03, March 2026

referenced validated methodology.

3.1.4 Damping System and Bolted Connections (Conceptual Representation)

The cabin assembly includes a four-spring damping unit and bolted interfaces at the support junctions, as described in the reference configuration in [6]. In the present work, the structural evaluation has focused only on the critical components the floor frame, H-bracket and coupling element support “H”. Consequently, detailed analytical calculations of damping forces and bolt preload have not been performed.

Instead, the functional effects of these subsystems have been represented through boundary conditions in the finite-element model. The damping system has been idealized by applying translational restraints consistent with the stiffness contribution of the springs, while the bolted joints have been modelled using fixed or pinned constraints to simulate load transfer at the interfaces. This representation has allowed the essential mechanical behavior of the damping and connection systems to be included in the analysis without extending beyond the scope of the current structural study.

3.2. Type of Loads and Load Combinations

The structural analysis of the ten-passenger cabin is conducted under combined loading conditions defined in UNE-EN 13796-1 [1] and following the methodology adopted in [6]. The applied loads comprise the self-weight of the cabin (G), non-structural component load $(G1)$, passenger load (Q), wind (F_W), hail (S), dynamic reaction (R) and partial passenger load (QP). These load magnitudes correspond to those calculated for the present design (Section 2.1).

Six governing combinations have been considered to capture the most critical operating conditions, consistent with the referenced methodology:

(1) $G + G1 + Q + FWx\,(+)\ + S,$

(2) $G + G1 + Q + FWy\,(+)\ + S,$

(3) $G + G1 + Q + FWy\,(-)\ + S,$

(4) $G + G1 + Q + S,$

(5) $G + G1 + 0.5Q + R + S,$

(6) $G + G1 + QP.$

The expressions used for dead and passenger loads follow basic weight calculations, wind load is obtained from the standard wind pressure relation, hail load is estimated from its density and accumulation height, and the dynamic reaction force is evaluated using Newton’s second law, in accordance with relevant design codes [1], [2], [9]. Combinations (1)–(3) evaluate wind effects in both longitudinal and transverse directions, including reversal. Combination (4) represents the static case without wind; combination (5) incorporates the transient dynamic reaction during station entry and combination (6) simulates uneven passenger distribution. These load cases have been implemented to determine the governing stress and deformation states of the aluminum cabin structure and the steel support bracket, with all results verified against the safety requirements of UNE-EN 13796-1 [1].

IV. RESULTS AND DISCUSSION

All structural analyses have been carried out in ANSYS R1 2024 under static conditions. The cabin static loading conditions defined in section 2. $Aluminium\ Alloy\ 6061 - T6$ has been used for the cabin frame and coupling element support ‘H’, while H-bracket has been modeled using ASTM A572 Gr50 steel. The finite element models have been developed using appropriate mesh densities and element formulations to ensure accurate representation of stiffness, deformation patterns and stress behavior in each structural component.

The results presented in the following subsections include deformation contours, von Mises stress fields and safety factor distributions for the three major assemblies of the cabin system. These outputs demonstrate the structural adequacy of the design and provide insight into the load-transfer characteristics of the floor frame, H-bracket, and coupling element support ‘H’.

4.1. Floor Frame Structure Analysis

The floor frame structure has served as the main load-carrying component of the cabin, transmitting passenger and equipment loads to the supporting frame and H-bracket. $The\ Aluminium\ 6061 - T6\ (E = 69\ GPa, \nu = 0.33,$ $\sigma_Y = 275\ MPa)$ has been used for the floor Frame. The frame, consisting of longitudinal and transverse stiffeners has been modeled using two-dimensional surface elements to assess deformation and stress response under the governing load combinations defined in [1]. Boundary conditions have been applied at the four coupling points connecting the floor to the support bracket ‘H’, where each point has been fixed against translation in (X, Y, Z) directions, while rotation have been left free, representing a pinned-type connection that restricts linear displacement but allows limited rotational flexibility of the cabin base.

A uniform pressure load has been applied to the entire floor surface to represent the combined dead load and passenger load of ten occupants (80 kg each), producing a total force of 12,740 N. Over the effective floor area of $2.55\ m \times 1.40\ m\ (3.57\ m^2)$, this corresponds to a pressure intensity of $3.57 \times 10^{-3}\ MPa$, acting in the downward direction.

ISSN (Online) 2456-1290

International Journal of Engineering Research in Mechanical and Civil Engineering (IJERMCE)

Volume 13, Issue 03, March 2026

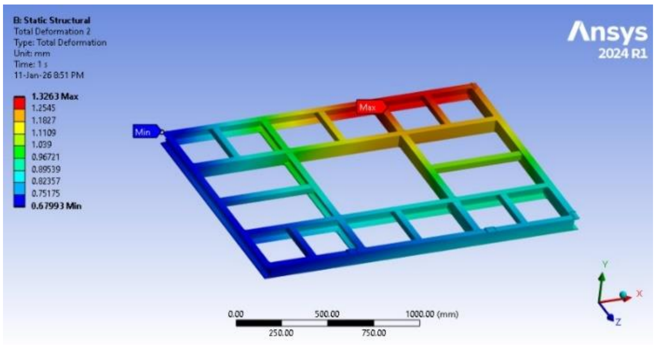

Figure 2. Maximum deformation of the cabin floor structure

The analysis has shown a maximum deformation of 1.326 mm at the central region of the floor frame (Fig. 2). The peak von Mises stress, illustrated in Fig. 3, has reached 46.79 MPa along the intersections of the stiffeners. The minimum safety factor has been found to be 5.89, indicating that the structure remains safely within elastic limits. These results have remained consistent with the behavior reported for similar cabin configurations in [6] and satisfy the safety provisions of UNE-EN 13796-1 [1].

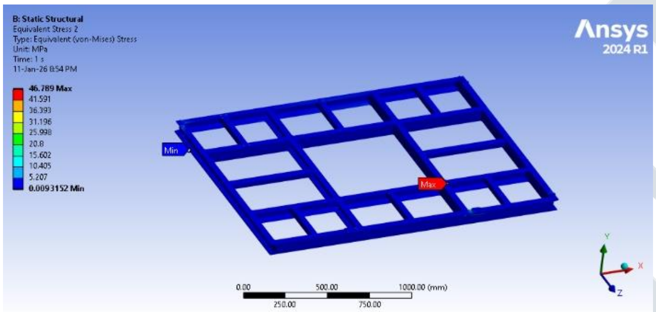

Figure 3. Von Mises equivalent stress of Cabin Floor Structure

4.2. Coupling Element Support 'H'

The coupling element support 'H' has served as the primary structural interface between the cabin frame and the H bracket. It transmits both static and dynamic reaction forces that develop during operation, particularly when the cabin accelerates or decelerates within the station approach zone as defined in [1], [6]. The component has been modeled using solid structural elements to capture its deformation and stress response under the governing load combinations. Boundary conditions have been applied by fixing the bottom surface of the base plate in all translational degrees of freedom (X, Y, Z). A concentrated vertical load of 3,185 N has been applied at the upper face of the H-support to simulate the coupling reaction transmitted from the cabin frame. This load corresponds to one-fourth of the total operational load of 12,740 N, reflecting the load-sharing approach adopted in [6].

The analysis has indicated that the maximum total deformation occurs at the upper joint region, with a magnitude of 0.3101 mm, as illustrated in Fig. 4. The von Mises stress distribution, presented in Fig. 5, shows a maximum stress of 51.85 MPa, remaining well below the yield strength of Aluminum 6061-T6. The corresponding minimum safety factor has been obtained as 5.52, confirming that the coupling element operates safely within the elastic range.

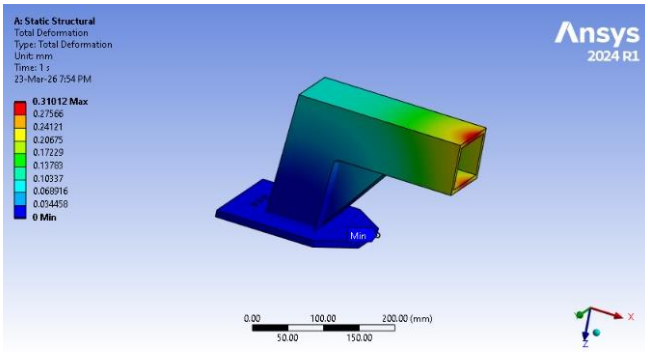

Figure 4. Maximum Deformation of Coupling Element support 'H'

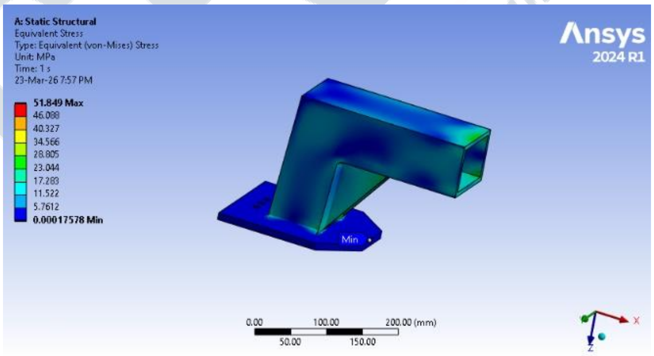

Figure 5. Von Mises equivalent stress of Coupling Element support 'H'

4.3. H Bracket Analysis

The H-bracket has served as the connecting component between the cabin frame and the supporting chassis, transmitting the combined loads from the cabin structure to the ropeway support system. The applied loading has been represented as a combination of static, environmental and dynamic effects as defined in eq. 6 & expressed as:

$$F_{total} = G + G1 + 0.5Q + R + S \quad (6)$$

following the procedure adopted in [6]. For the present cabin, the total load has been computed as 18,306.4 N, which has been distributed equally among the four support points, resulting in an effective reaction of approximately 4,576 N per support.

IFERP
Explore Your Research Journey...
ISSN (Online) 2456-1290
International Journal of Engineering Research in Mechanical and Civil Engineering (IJERMCE)
Volume 13, Issue 03, March 2026

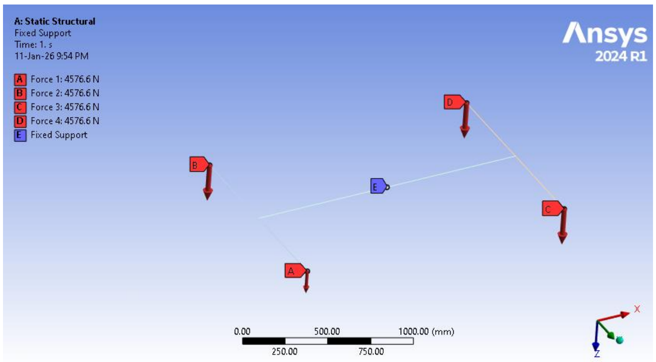

Figure 6. Boundary condition and applied loading on the H-bracket

The H-bracket has been designed using ASTM A572 Gr50 steel, having an allowable design stress σ_{adn}= 345 MPa. The bending moment distribution has indicated two critical regions at the central and lateral profiles. The maximum bending moment has been determined as $M_{max} = 7.7802 \times 106\ \mathrm{N \cdot mm}$ for the central profile, M_{max} =2.7002×106 N·mm for the lateral profile. The corresponding bending stresses and safety factors have been evaluated using eq. (7) and (8):

$$\sigma b = \frac{M_{max}}{S2-2}, \quad (7)$$

$$n = \frac{\sigma_{adn}}{\sigma b} \quad (8)$$

The bending stress and corresponding safety factor have been evaluated using standard mechanical design relations presented in [9].

The geometric and mechanical properties used in these evaluations are summarized in Table 1, and the resulting bending stresses and safety factors are presented in Table 2.

Table 1. " H " Bracket profile

Element	Dimension (mm)	Length (mm)	Cross section Area (mm^2)	Section Module (mm^3) -Axis 2-2
Central profile	150 × 150 × 6	1700	3456	159528.96
Lateral profile	100 × 70 × 6	1220	1896	40786

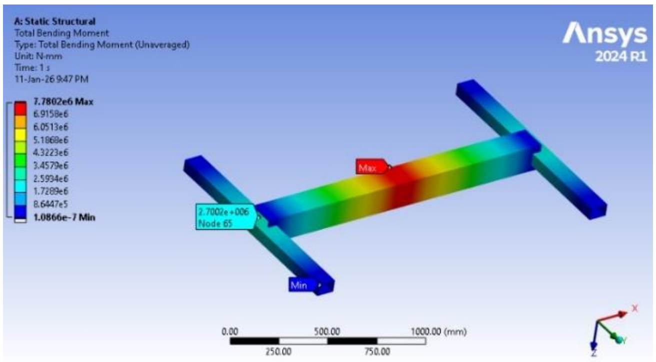

Figure 7. Total Bending Moment of central and lateral Profile

Table 2. Calculation of Bending Stress and Factor of Safety

Profile Type	M_{max} (N·mm)	S_{2-2} (mm^3)	σb (MPa)	σ_{adn} (Mpa)	N(FOS)
Central profile	7.7802×10^6	159528.96	48.76	345	7.07
Lateral profile	2.7002×10^6	40786	66.20	345	5.21

The results have shown that both profiles operate safely within the allowable stress limits of ASTM A572 Gr50 steel. The calculated safety factors are higher than the acceptable limits reported by Villarreal et al. [6] and indicate that the structural components satisfy the safety requirements specified in UNE-EN 13796-1 [1], with 7.07 for the central profile and 5.21 for the lateral profile. These values have demonstrated that the H-bracket possesses adequate stiffness and strength to withstand the combined loading conditions.

V. CONCLUSION

The structural design and validation of a ten-person aerial transport cabin have been successfully carried out through finite element analysis in accordance with UNE-EN 13796-1 [1]. All governing load conditions including passenger load, permanent masses, wind action, hail impact and dynamic reaction forces have been incorporated to ensure realistic operational performance. The cabin frame, floor assembly, H-bracket, and coupling element have exhibited low deformation and moderate stress levels with safety factors that remain well above the minimum requirements specified in the standard.

In comparison with the reference configuration presented in Villarreal et al. [6], the present cabin has demonstrated improved stiffness, higher safety margins and a more uniform distribution of stress across critical members, while maintaining a lightweight structural layout. The maximum deformations observed in the floor frame and coupling element have been significantly lower than those reported in [6], confirming that the updated design has ensured better load transfer and strengthened structural efficiency.

ISSN (Online) 2456-1290

International Journal of Engineering Research in Mechanical and Civil Engineering (IJERMCE)

Volume 13, Issue 03, March 2026

REFERENCES

[1] UNE-EN 13796-1, *Cableway installations designed to carry persons – Safety requirements – Part 1: Cabins, doors, windows, ventilation and glazing*, AENOR, Madrid, 2017.

[2] NEC-SE-CG, *Norma Ecuatoriana de la Construcción – Cargas en General*, Instituto Ecuatoriano de Normalización (INEN), Quito, Ecuador, 2014.

[3] ASTM A572/A572M-18, *Standard Specification for High-Strength Low-Alloy Columbium-Vanadium Structural Steel*, ASTM International, West Conshohocken, PA, 2018.

[4] Haigermoser, C., & Kühn, M., "Wind effects on ropeway cabins," Journal of Wind Engineering and Industrial Aerodynamics, 2016.

[5] UNE-EN 12929-1, *Safety requirements for cableway installations designed to carry persons – Part 1: General requirements, 2015.*

[6] P. Villarreal, P. Caza, V. Macha, and V. López, "Design of an Aerial Cable Transport Cabin," in *Advances in Intelligent Systems and Computing*, vol. 1277, pp. 491–504, Springer Nature Switzerland AG, 2021.

[7] *EMMOP, Estudio Hidrometeorológico Regional de Quito, Empresa Metropolitana de Movilidad y Obras Públicas, Quito, 2016.*

[8] S. Agarwal and R. Singh, "Finite element analysis of passenger cabin structure for ropeway systems," *International Journal of Mechanical Engineering and Technology*, vol. 10, no. 4, pp. 132–140, 2019.

[9] J. E. Shigley and C. R. Mischke, *Mechanical Engineering Design*, 10th ed. New York: McGraw-Hill Education, 2015.

[10] Haigermoser, A., & Kühn, M. (2016). Ropeway engineering – Fundamentals and design guidelines. Springer Vieweg, Wiesbaden.

[11] K. Hoffmann and R. Liehl, "Oscillation effects of ropeways caused by cross-wind and other influences," FME Transactions, vol. 37, no. 4, pp. 175–184, 2009.

[12] J. M. W. Brownjohn, "Dynamics of an aerial cableway system," Engineering Structures, vol. 20, pp. 826–836, 1998.

[13] J. Guštinčič and L. M. García Raffi, "Analysis of oscillations in a cableway: Wind load effects," in Proceedings of the International Conference on Cableway Transport Systems, Valencia, Spain, 2013.

[14] M. Lenti, G. Pomaranzi, P. Schito, and P. Pennacchi, "Dynamics of an aerial cableway through a time-varying meshing finite element approach," Mechanics Based Design of Structures and Machines, 2025.

[15] Arena, B. Carboni, W. Lacarbonara, and M. Babaz, "Nonlinear dynamic response of ropeway roller batteries and cabin assemblies in bi-cable gondola systems," Nonlinear Dynamics, vol. 104, no. 2, pp. 1457–1475, 2021.

[16] Hoyos E, Serna MC, Gutiérrez S, Montoya Y, Córdoba JH, Palacio ME and Álvarez I. Assessment via finite element analysis: Cable cart system elements manufacturing feasibility. *Advances in Mechanical Engineering* 2024; 16(12): 1–11.